Journal of Scientific & Industrial Research
Vol. 81, June 2022, pp. 671-682

Effect of Green Processing on Enhancement of Thermal Conductivity of Nanofluid for Thermal Applications

Jayashree Sa and Ganeswar Nath*

Department of Physics, Veer Surendra Sai University of Technology, Sambalpur 768 018, Odisha, India

Received 10 December 2021; revised 14 May 2022; accepted 17 May 2022

Thermal tuning properties of nanofluid from lower to higher value is a challenging issue in the field of thermal industries and microelectronic industries as well as in medical sciences. Nanofluids of aluminum oxide has been prepared with different volume fraction varies from 0.01– 0.05 vol%. The crystal structure and surface shape of the synthesized aluminum oxide nano powder has been studied using X-ray diffraction technique (XRD), scanning-electron-microscopy (SEM) and electron transmission microscopy (TEM). The nanofluids are characterized by experimental technique such as FTIR, UV-visible, photoluminescence and particle distribution with particle size analyzer. Thermal conductivity of the alumina nano fluid was found to vary from 0.5378–0.7299 W/mK for volume percentage 0.01–0.05 respectively with enhancement from 1.8 % to 21.44% which is better than other works in the literature. With increase of sonication time, thermal conductivity varies appreciably from 0.531–0.736 W/mK with volume fraction of nanofluid. This significant increase in thermal conductivity of alumina nanofluid in different operating condition may be attributed to extraction and oxidation of alumina nitrate assisted with leaf extracted surfactants.

Keywords: Alumina nanofluid, Green synthesis, Thermal conductivity, Ultrasonic wave

Introduction

Successful utilization of energy and its management is always a challenging issue in 21st century for progress in technology and the development of industries. Thus triumphant features of heat transfer fluid called nanofluid clear its importance as an efficient and sensitized material for modern industries and nanotechnology. Recent advances in heat processing industries, cooling industries including manufacturing units like air conditioning and refrigeration systems, thermal storage systems, electronic cooling systems, and others are some of the important sector applications where heat transfer fluid plays an important role. Many industries ranging from macro to nano, space science, and medical science require ultrahigh performance cooling as an efficient consideration for different mechanisms and processes.[1]

The rapid activity of nanomaterials and their fluid form plays an important role in thermal industries and surface science for various applications in designing advanced materials in fast operating devices.[2–4] They further attract researchers for advanced work on nanofluid. Being a smart material, nanofluid emerges as a new kind of energetic component for an ultrafast device with a size in nanoscale range that varies from 1–100 nm within a base fluid. The traditional problems like corrosion, cohesion, and sedimentation of heterogeneous materials are not only solved by the inclusion of this nanofluid but also enormously increase the thermal efficiency of the base fluid for holding nanoparticles. Though there are many investigations on thermal conductivity of different metals with a base fluid-like ethylene-glycol nanofluid, with water as the base fluid has high significance than other base fluids.[5]

The anomalous behavior and the holding capacity of water recognize its suitability as the base fluid for many metallic particles which form the metal-based nanofluid. The presence of oxygen in water accelerates the oxidation processes for synthesizing different nanoparticles and finally increases the growth of nanoparticles by enhancing the chemical reactivity.[6] Water is an excellent choice for liquid cooling applications because of its high heat capacity and thermal conductivity. Water is employed as base fluid in much of the work in green synthesis because thermal conductivity is constantly increasing. This is owing to the huge number of H-bonds found in water molecules, which can store energy rather than transfer it.

*Author for Correspondence
E-mail: ganeswar.nath@gmail.com

Alumina has grabbed researchers' interest among the newly developed nanomaterials because of its unique chemical and physical properties, which are basically thermal properties. Alumina, in particular, has shown to have strong heat resistance, thermal conductivity, and heat transfer coefficient qualities. As a result, alumina has been tested in a variety of disciplines for its value, significance, and efficiency. As the third most abundant component in the Earth's crust, aluminum has a wide range of uses in automobiles, aircraft, aircraft heat-protective coatings, rust, defence applications, and more importantly, its unique and challenging properties have the potential to store high hydrogen. Further, the alumina particle of nano-size becomes more significant in various thermal and electrical applications due to its high ability to enhance thermal conductivity when it is impregnated in a suitable environment.

In reality, though several studies have described the use of nanoparticles in various thermal devices to improve thermal conductivity, still multiple challenging issues arise on account of the stability of nanofluid, method and root of synthesis of nanoparticle and faulty mechanism in explaining the nanoparticles interaction with base fluid systems.[7] The green synthesis approach of nanoparticles involves the use of plant extract because this method of synthesis is mentioned at ambient temperature, neutral pH, cost-effective, and eco-friendly without emission of any toxic gas to the environment. Moreover, green technology of nanoparticle synthesis involves two major concepts such as (i) as solvent water must have to use and (ii) a natural source/extract is utilized as the main component. The evergreen thermal enhancement properties of metal nanofluid have enriched its significance in different technology and industries due to its unique characteristics such as dispersion and stability.[8]

The propagation of a high-frequency ultrasonic wave through a specified regime in nanomaterial and an interfacial layer of nanofluid brings the undistinguished properties in maintaining stability and thermal enhancement of metallic nanofluid. Being a powerful nondestructive technique its interaction with nanofluid provides many physicochemical properties of nanomaterial in achieving optimal applications in different scientific mechanisms and formulations.[9] Thermophysical properties of a water-based alumina-graphene nanofluid was found to be 4.23% enhanced with temperatures ranging from 20–40°C.[10] Thermo-physical properties of TiO_2, Al_2O_3, and SiO_2 nanofluids with volume concentrations of 0.05–0.5 % at temperatures ranging from 25–40°C was found to be 15% with increase in heat transfer coefficient.[11] Thermo-physical properties of water and ethylene glycol based Al_2O_3 nanofluids of volume concentration 0–1 vol% within temperature range of 10–50°C was studied and observed that the thermal conductivity of the nanofluids increased with the increase of volume concentrations.[12]

The current study combined the synthesis of alumina nanoparticles with the green mechanism of *Murraya koenigii* plant leaf extract and ultrasonic wave impregnation in each phase of the synthesis. The thermal conductivity of the produced alumina nanoparticles is very high for a relatively small concentration of nanoparticles in base fluid water, which supports the findings of the literature. The characterization of nanoparticles by different experimental techniques, and factors causing enhancement of thermal conductivity is significantly validated the importance of water-based alumina nanofluid for thermal applications.

Experimental Method

Materials

Curry leaves (*Murraya koenigii*) were collected locally and processed forits leaf extract which serve as both stabilizing and reducing agents. Aluminium nitrate has been used as precursor for the formation of alumina nanoparticles. The synthesis of nanofluid was done in two steps, alumina nanoparticles were first synthesized and then alumina nanofluids were prepared with distilled water.

Preparation of Aluminum Oxide Nanoparticles

Preparation of Leaf Extract

Curry leaves (*Murraya Koenigii*) were cleaned with distilled water after being freshly chopped. The small pieces of curry leaves were boiled with distilled water for 30 minutes followed by cooling at room temperature was centrifuged for 15 minutes at 3500 rpm (REMI-R-8C laboratory centrifugal machine) for preparation of curry leave extract. After that the plant extract was filtered using the filtration process through a 0.45 µ Whatman filter paper. The filtrates were kept at 5–10°C in a cone-shaped flask.

Synthesis of Alumina Nanoparticles using Curry Leaves Extract

Aluminum oxide nanoparticles were synthesised using aluminium nitrate as a precursor. In a conical flask

at a constant temperature of about 50°C, an aqueous solution of 0.01M aluminium nitrate was mixed in an aqueous leaf extract of curry leaves in the ratio 1:1. The sample was placed in a magnetic stirrer (1500 rpm) for about 1 hour, or until it turned yellowish-brown. After centrifuging for 30 minutes at 3500 rpm, the precipitate was washed with distilled water.

To guarantee effective separation of alumina particles, the centrifugation and re-dispersion process was done 5 to 6 times in sterilized deionized water. The purified particle sediment was then dried for 12 hours at 50°C in an oven.

Preparation of Alumina Nanofluid

Distilled water was used as the base fluid for the alumina nanofluid preparation. We used an ultrasonic bath Sonicator and a magnetic stirrer to make nanofluid in various concentrations such as 0.01, 0.02, 0.03, 0.04, and 0.05 vol%. At first, 3.9 mg alumina nanopowder was weighted and added to 100 ml water in a 150 ml beaker containing 100 ml water. Because of its hydrophobic nature, Al_2O_3 does not dissolve in water. The solution was kept in an ultrasonic bath Sonicator for 60 minutes. The sonication effect provides high-frequency sound waves that enable nanoparticles to diffuse well into the base fluid for well dispersion. The solution was then stirred with a magnetic stirrer (1500 rpm) for 30 min followed by cooling and storage in an airtight container that is free of moisture. The process was repeated for different concentrations like 0.02, 0.03, 0.04, and 0.05 concentrations of nanofluid. The agglomeration of

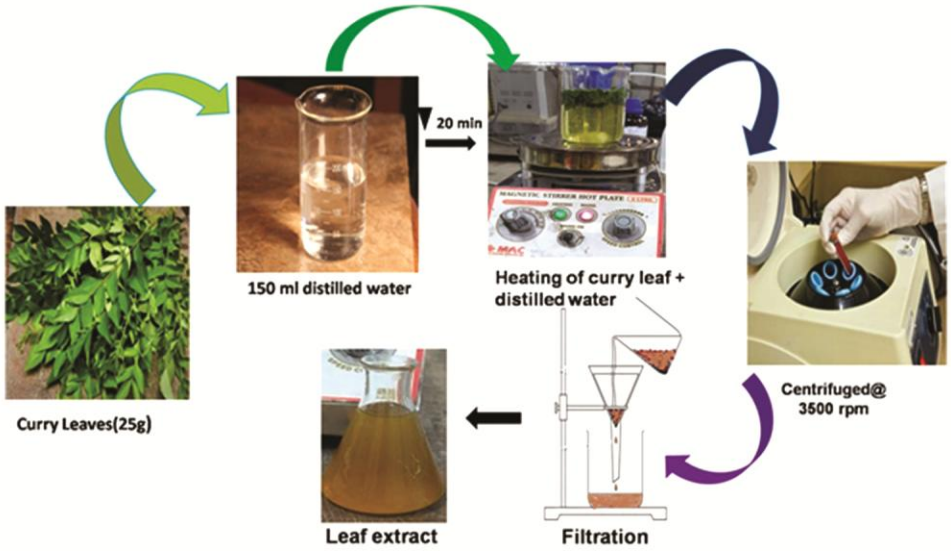

Fig. 1 — Preparation of leaf extract

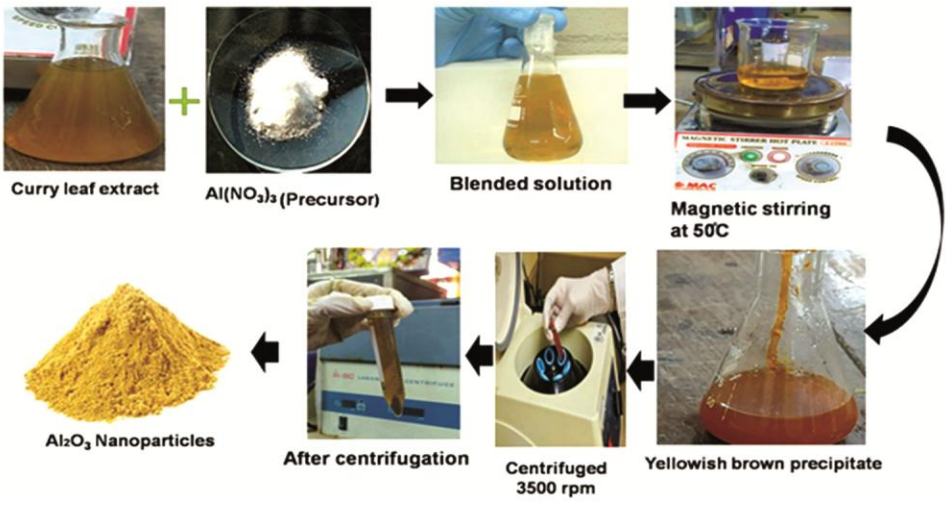

Fig. 2 — Green synthesis of alumina nanoparticles from $Al(NO_3)_3$ using leaf extracts

nanofluid was avoided with the process of sonication and magnetic stirring that enables the powder particle to disperse properly in the base fluid. The systematic steps for the preparation of nanofluid are described in Fig. 3.

Characterization of Alumina Nanoparticle

BRUKER D8 ADVANCE was used to identify the crystalline structure of alumina nanoparticles using the powder X-ray diffraction (XRD) method. The diffractometer was discovered using a CuKα X-ray source with a wavelength of 1.54A°, where Cu is used as an anode material. The diffractograms were taken at a fixed diverging slit at 10° with 2θ variations from 10–80°. The X-ray tube's current and voltage were set to 30 mA and 40 kV, respectively. The crystalline structure of alumina nanoparticles as well as the pattern of peaks were studied using PANalytical X'PertHighscore software. Surface morphology of alumina nanoparticles was performed by SEM operating at 5 kV at pressure of 0.1 torr and current of 18 mA. A transmission electron microscope (ZEISS EM-900, 80 kV) is used to analyze the aggregation of nanoparticles within the base fluid. FTIR spectra of KBr pellets were acquired using a (Bruker alpha-II USA) FTIR spectrometer in transmittance mode in the wave number range of 4000–500 cm^{-1}. The UV-Vis spectrometer (UV-19001) was used to record the optical absorption spectra at room temperature.

Experimental Measurement in Nanofluid

A nondestructive technique like ultrasonic measurement has been performed in the analysis of physicochemical properties of nanofluid. Experimental measurement of ultrasonic velocity has been performed which explains different inter and intermolecular interactions between Al_2O_3 and water nanofluid. The present investigation encompasses the ultrasonic-based computation of thermal conductivity of Al_2O_3 and H_2O nanofluid and the experimental measured thermal conductivity with different operating conditions. The pycnometer was used for the measurement of the density of nanofluid in different concentrations with varying temperatures controlled by a water circulation bath. High precise balance was employed for the determination of weight in preparation of exact concentration of nanofluid with an accuracy of ± 0.1 mg. A Digital nanofluid interferometer was used for the determination of ultrasonic velocity in pure water as well as in alumina nanofluid with varying concentrations with an accuracy of 0.1 m/s. The density of alumina nanofluid was measured using the mass balance formula given by

$$\rho_{nf} = (1-\varphi)\rho_{bf} + \varphi\rho_p \quad \ldots (1)$$

where, φ is the volume concentration of nanofluid. The viscosity of alumina nanofluid was measured at different temperatures using a Redwood viscometer. The thermal conductivity of alumina nanofluid was

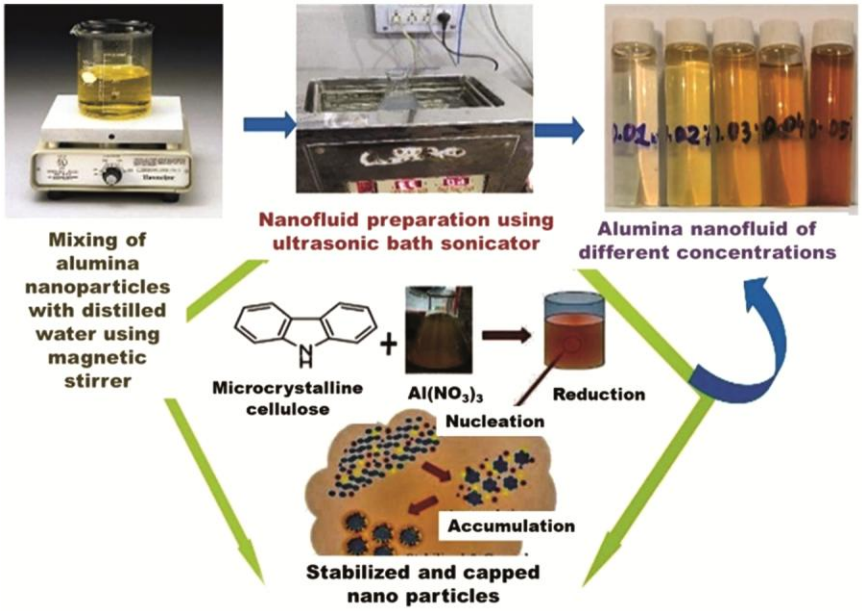

Fig. 3 — Alumina nanofluid preparation method

measured by the TEMPOS thermal analyzer where KS-3 sensor is inserted into the sample bottle placed in a calorimeter arrangement at different temperatures for various vol%. The percentage enhancement in thermal conductivity of nanofluid was calculated using Eq. (2),

$$\%K_{Enha} = \frac{K_{nf} - K_{bf}}{K_{bf}} \times 100 \quad \ldots (2)$$

Results and Discussion

Formation of nanocrystalline phase was confirmed using XRD data analysis of green synthesized alumina nanoparticles. The traces of aluminium oxide are confirmed from diffractograms peak pattern at (25.6°, 35.1°, 37.8°, 43.3°, 52.5°, 57.5°, and 68.2°) with increasing intensity of X-ray beam. The peaks are indexed with miller indices ((0 1 2), (1 0 4), (1 1 0), (1 1 3), (0 2 4), (1 1 6), (3 0 0)) as shown in Fig. 4. The lattice space group- R-3c with cell parameters a = 4.7580, b = 4.7580, and c = 12.9910 confirms the rhombohedral structure of aluminium oxide traces. In order to confirm the nanoscale size of aluminium oxide, the particle size (grain size) was calculated using the Debye-Scherer formula.

$$D_{hkl} = \frac{k\lambda}{\beta_{hkl} \cos\theta_{hkl}} \quad \ldots (3)$$

where, D_{hkl} is the average crystallographic size of reflected phases, k is Scherer's constant having value 0.9; λ is the X-ray wavelength which is 0.154 nm, β_{hkl} is the full width half maximum (FWHM) intensity, and θ_{hkl} is the Bragg's angle. From the calculation, it is reported that the crystalline size ranges between 10−72 nm. Further, to confirm the nanoparticle phase, the degree of crystallinity was calculated and found to be 46.87% which indicates that the synthesized samples of alumina nanoparticles are amorphous in nature. The SEM analysis of the synthesised alumina nanoparticle indicates spherical shape of 38 nm size with agglomerations between them, as shown in Fig. 5.

Further, it is observed that this agglomeration takes place due to the formation of a cluster of spherical-shaped nanoparticles composed of a grain of maximum diameter 3.12 nm as observed peaks in the distribution of particles. After annelation of the aluminium oxide nanoparticle, EDS was performed for chemical compositions keeping reference peak at 0 KeV. From the spectrum analysis, it was observed that aluminium and oxygen were present with 38 atomic wt% and 62 atomic wt% synthesized by the curry leaf extraction process.

Bath sonicated Al_2O_3 nanofluids are analysed using TEM to study the effects of ultrasonic irradiation on alumina nanoparticle dispersion in the base fluid. The shapes of nanoparticles are spherical (Fig. 6) and particle sizes have risen due to agglomeration caused by cohesive force[1], according to the TEM image.[13]

The exact information of different functional groups exist in processing of alumina nanoparticle synthesized through curry leaf treatment on alumina nitrate can be well analyzed by the spectra of FTIR as shown in Fig. 7. The reducing action of several phytochemicals converts simple inorganic aluminum nitrate to aluminum oxide which serves as a stabilizing and capping agent. The broad peak at 3436 cm^{-1} and 3220 cm^{-1} in the spectra corresponds to

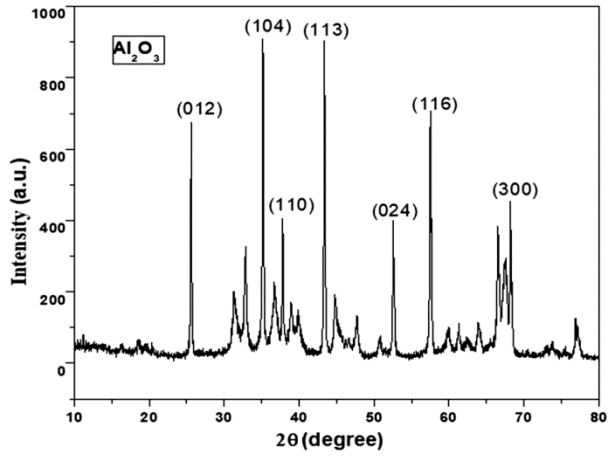

Fig. 4 — X-ray diffraction spectra of synthesized alumina nanoparticle

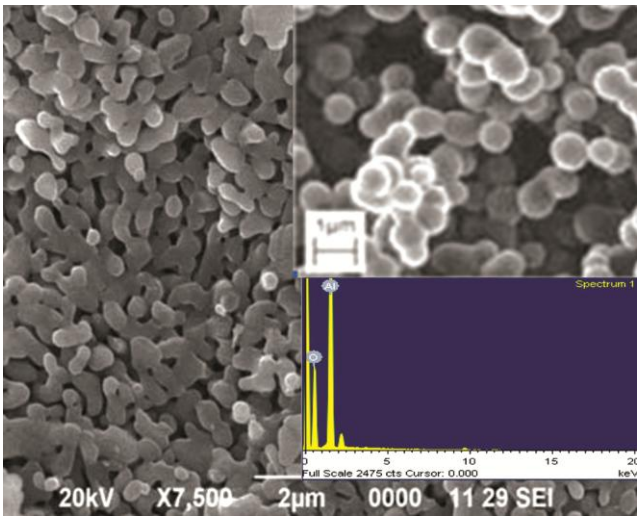

Fig. 5 — SEM and EDS image of alumina nanoparticle

the O-H stretching vibration of water molecules which is constituent of the base fluid. The bending vibration of water molecules (O-H) is represented by the peak at 1672 cm^{-1} possibly due to moisture absorbed by the nanoparticles. The peaks from 1384 –1134 cm^{-1} are observed due to the presence of an N-O bond which is possibly formed due to $Al(NO_3)_3.9H_2O$ precursor. The peak at 604 cm^{-1} is due to the production of Al-O-Al bonds. The production of Al_2O_3 nanoparticles is confirmed by transmittance peaks ranging from 1384 to 604 cm^{-1}. The spectroscopic studies of the sample were performed in presence of ultraviolet light for stability analysis as well as to establish the optical and structural properties of the alumina nanomaterials. The samples of each concentration were scanned in the presence of UV-visible light in the wavelength range 200–400 nm.

The strong absorption peak for all the synthesized samples was obtained (λ_{max}) at 238 nm as shown in Fig. 8(a) which confirms the existence of alumina nanoparticles in the suspension as well as an agreement with the published result.[14] Nanoparticles with a diameter of 10 nm are approximate to the peak of about 200 nm.

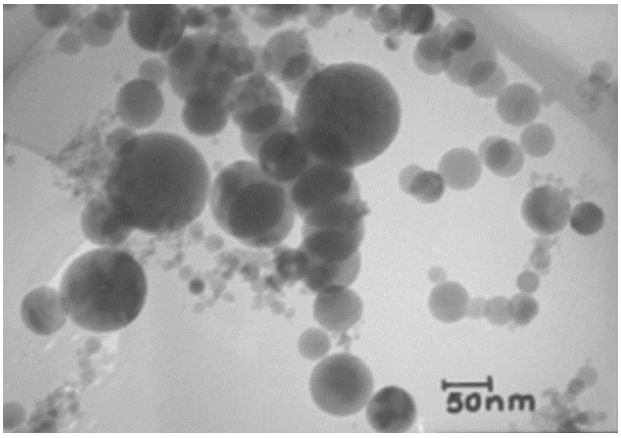

Fig. 6 — TEM image of alumina nanoparticle in water

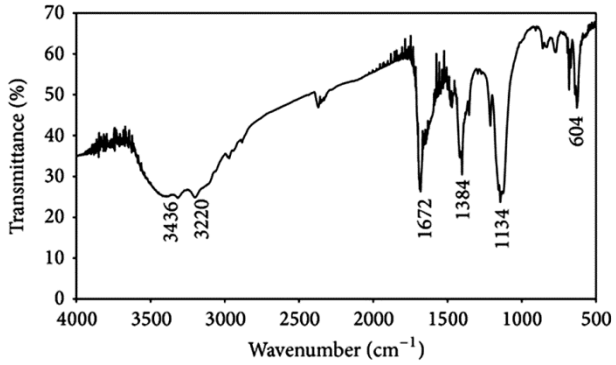

Fig. 7 — FTIR spectra of green synthesized alumina nanopowder

As the peaks of all the samples are located at 238 nm, this is in confirmation with the fact that there is no further change of size of the nanoparticle even if the sample was tested three more times at three to four months later. This confirms the stability of nanoparticles within the suspension and dependence of absorption peak on the size nanoparticles in nanofluids.[15] The optical bandgap of Al_2O_3 nanoparticles was calculated using general electron transition events from the valence to conduction bands. The Wood and Tauc[15] equation was used to get the optical energy bandgap (E_g) by:

$$\alpha h\nu = C(h\nu - E_g)^n \quad \ldots (5)$$

where, α is absorption coefficient, h is the Planck's constant, ν is the frequency of ultraviolet light, C is the energy-independent constant, E_g are optical energy band-gap and n are related to a constant variety of electronic transitions like n =1/2 for directly allowed, 2 for indirectly allowed, 3/2 for directly forbidden, and 3 for indirectly forbidden transition.[15] The direct optical band gap of the Al_2O_3 nanomaterial was evaluated by plotting the graph between $(\alpha h\nu)^2$ vs. (hν) as shown in Fig. 8(b). Extrapolating the linear portion of the curve the optical band gap of Al_2O_3 nanoparticles was found to be increased from 4.8–5.82 eV which revealed the decrease in the particles as shown in Fig. 8(b).[16]

Fluorescence Spectroscopy Studies

Fluorescence emission spectra of Al_2O_3 nanofluid were recorded using Cary Eclipse Fluorescence spectrophotometer in the wavelength range 400–500 nm for different vol% concentrations at room

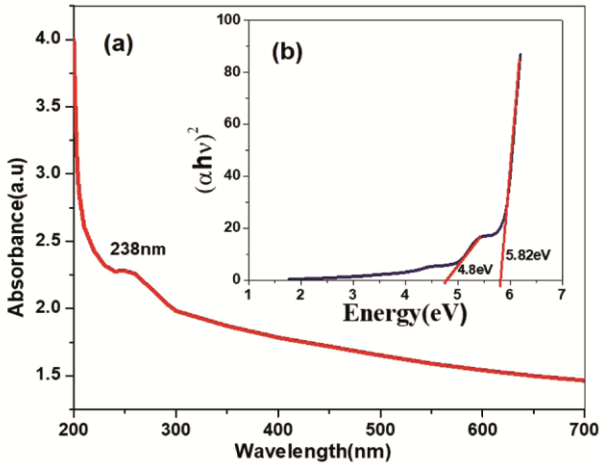

Fig. 8 — (a) UV-visible spectra of alumina nanofluid; (b) Energy bandgap from UV-Visible spectra

temperature as shown in Fig. 9. The excited molecules transmit to the lower energy state by losing the energy by emission of light with the collision of other molecules. From the spectra, it was observed that all the peaks are located around 456 nm which corresponds to violet emission caused by the radiating defects that occur at the interface traps existing at the grain boundaries.[17]

Particle Size Analysis of Alumina Nanofluid

The particle size distribution of water based alumina nanofluid was carried out using a Malvern Mastersizer -3000 equipped with an ultrasonic cleaner and a high-intensity laser source as illustrated in Fig. 10. As the alumina nanoparticles are synthesized from leaf extract which can act as both surfactants and stabilizing agents, there is only one strong peak was located in each concentration which indicates that there is a uniform distribution of particles.

Further, the particles of average diameter 3.12 nm are mostly distributed with all concentrations of nanofluid. The dispersity index of the nanofluids is determined by observing the variation of span with volume concentration in the spectrum. The lower value of the dispersity index indicates that conglomerate size consistency in nanofluids is better.

Measurement of Thermal Conductivity

As a key feature, the thermal conductivity of any nanofluid has a significant contribution to the designing of different sophisticated electronic devices used in nuclear reactor and space technology.[18] It has further diversification in heat pipes as heat exchangers, and storing of solar energy in solar cells[19] along with the improvement in diagnostic technique, drug delivery as used in medical science.[20] The different field of applications of nanofluid which are most relevant to thermal applications depends on the reduction and thermal optimization properties of the systems controlled by various parameters of the nanomaterials such as concentrations, shape, size, nature of base fluid and nanoparticle, temperature, preparation method, external stimuli like sonication time and magnetic field. The basis of hotwire method helps in the measurement of thermal conductivity very accurately, reliably, and quickly. The present work employed a TEMPOS thermal analyzer for measurement of thermal conductivity of alumina nanofluid based on hotwire principle using KS-3 sensor designed best for liquid sample with accuracy of ±10%. The KS-3 is a single needle sensor made up of stainless steel of 60 mm length and 1.3 mm diameter operated in a low-power mode with accuracy of ±10%. It was calibrated with glycerin before the measurement of thermal conductivity of the samples of nanofluid. The sensor is inserted perpendicularly within the nanofluid sample in a steady temperature bath to measure the thermal conductivity at different temperatures. The thermal conductivity of each sample was measured three times for more accuracy at each temperature. The recorded values of thermal conductivity are analyzed and discussed with a variety of different factors and plotted graphically.

The thermal conductivity of the Al_2O_3 nanofluid rises linearly with increase in nanoparticle concentration as shown in Fig. 11(a). The linear regression analysis for accuracy of thermal conductivity of nanofluid with volume% is shown in

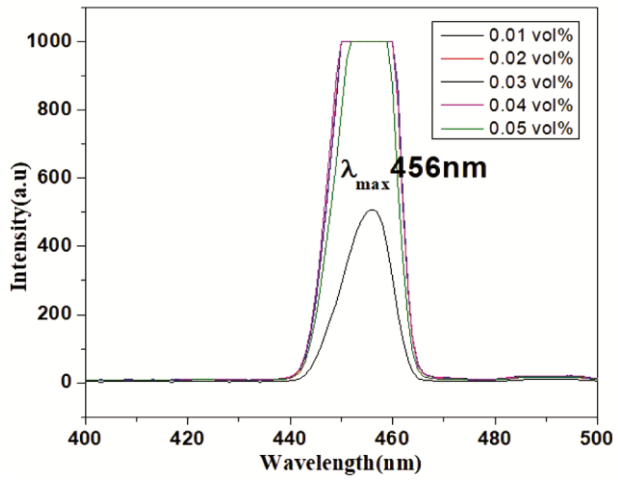

Fig. 9 — Photoluminescence spectra of Al_2O_3+H_2O nanofluids

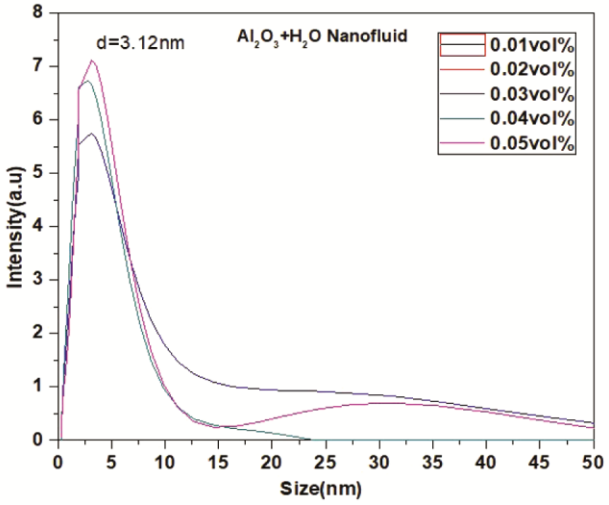

Fig.10 — Particle size distribution in Al_2O_3+H_2O nanofluids

Fig. 11(b). The coefficient of correlation (R^2) value is determined to be 0.9976. As the R^2 value is very much nearer to 1, the error fluctuations are very less.[21] From the nature of the plot, it is observed that the linear variation for every small volume fraction may be attributed due to the increase of agglomeration[22] between the nanoparticles and the stability of the nanoparticles in the base fluid. The agglomeration of nanoparticles results in a more particle-free area in the water with high thermal resistance. Further, at room temperature, the thermal conductivity increases linearly which may be attributed to more interaction at higher concentrations. This increase in thermal conductivity may be contributed to green processing of nanoparticles in which extract of curry leaves containing different phytochemicals which are acting as both stabilizing and reducing agents for holding the nanoparticles in base fluid supporting nano convention.[23] The different controlling factor-like type of phytochemicals and their concentration, pH, and the concentration of metals maintains the yield and their stability within the base fluid for enhancing the thermal conductivity of the nanofluid.[24] Though the shape of the alumina nanoparticles is spherical which has less capability in the enhancement of thermal conductivity but in the present work, it is observed that the thermal conductivity is appreciably increased as compared to the published works[25] by other methods of preparation. Further, this increase in thermal conductivity is supported by the fact that existence of a larger interfacial area between Al_2O_3 nanoparticles and the base fluid was due to the decrease in intermolecular distance between the nanoparticles.[26] As the temperature rises, the thermal conductivity of alumina nanofluids increases for varying concentrations of nanofluid, as illustrated in Fig.12(a). The linear regression analysis for accuracy of thermal conductivity of nanofluid with temperature for different volume concentration is shown in Fig. 12(b). The coefficient of correlation (R^2) value is

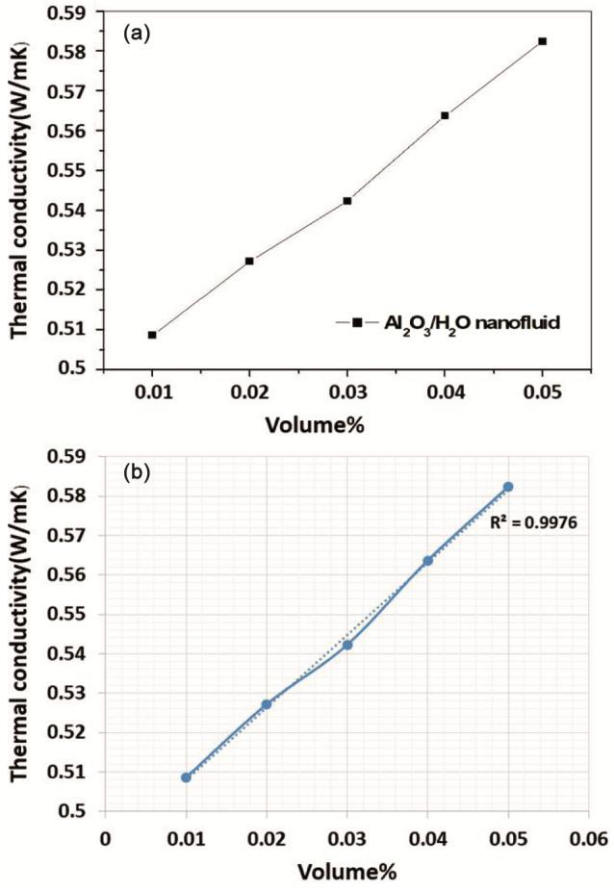

Fig. 11 — Representation of thermal conductivity vs. volume fraction (%) of nanofluids: (a) Variation analysis, (b) Regression analysis

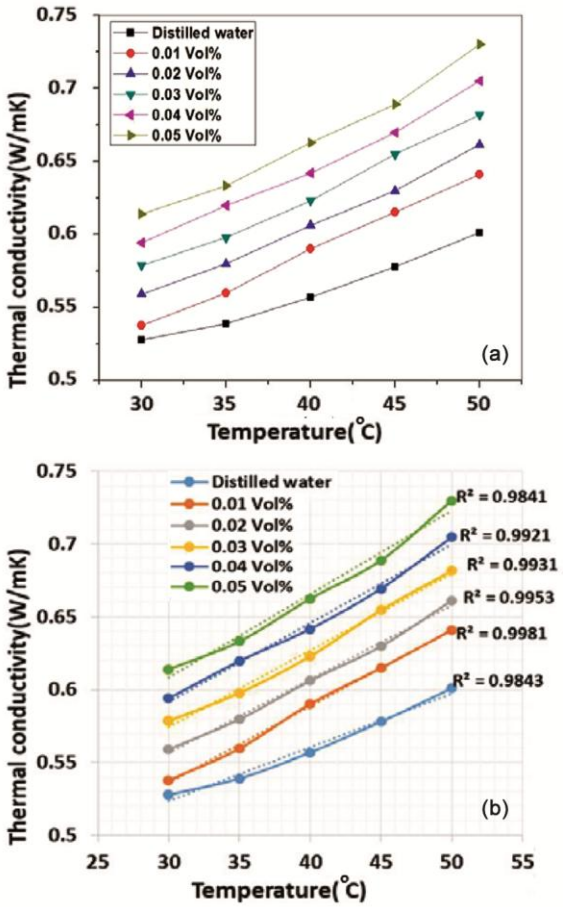

Fig. 12 — Representation of thermal conductivity vs. temperature: (a) Variation analysis, (b) Regression analysis

determined to be 0.9843, 0.9981, 0.9953, 0.9931, 0.9921, 0.9841 for distilled water percentage of 0.01, 0.02, 0.03, 0.04, and 0.05 respectively. As the R^2 value is very close to 1, the error fluctuations are very less.

The increment in thermal conductivity with volume fraction at different temperature is described in Fig. 13(a). The linear regression analysis for accuracy of percent increment in thermal conductivity of nanofluid with temperature for different volume concentration is shown in Fig. 13(b). The coefficient of correlation (R^2) value is determined to be 0.8759, 0.9298, 0.9575, 0.908, 0.9548 for 0.01%, 0.02%, 0.03%, 0.04%, and 0.05% respectively. As the R^2 value is very close to 1, the error fluctuations are very small. From the graph, it is observed that at 30°C temperature the thermal conductivity of nanofluid is more than the base fluid and with an enhancement of 1.85%–16.28% when nanofluid concentration varies from 0.01–0.05. With an increase

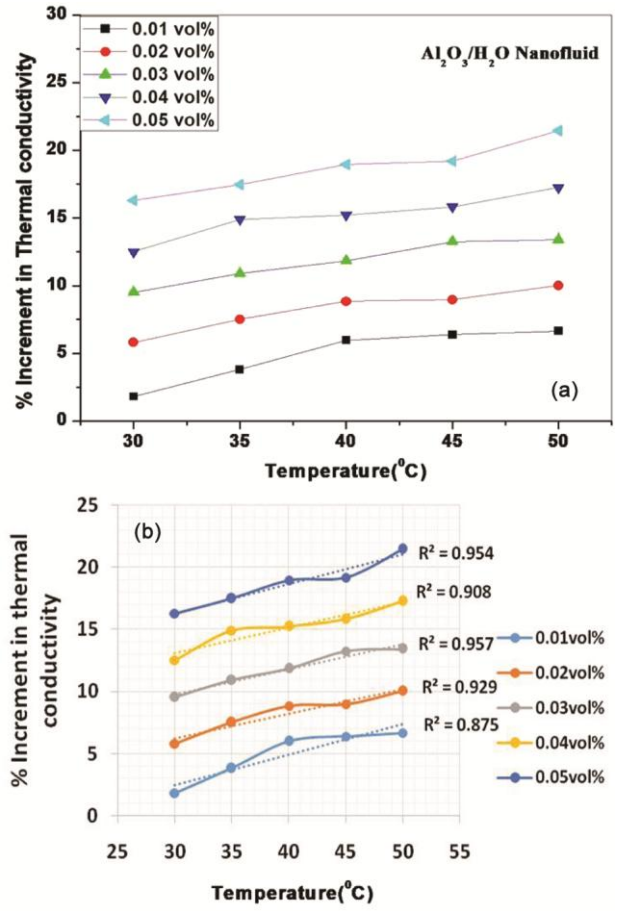

Fig. 13 — Representation of increment in thermal conductivity (%) vs. temperature: (a) Variation analysis; (b) Regression analysis

of temperature from 30–50°C enhancement in thermal conductivity is from 6.65%–21.44% which is found to be more in the present case as compared to literature.[27] This large increase in thermal conductivity could be explained by the fact that a higher concentration of nanoparticles enhances Brownian motion as temperature rises. As a result, micro convection's role to heat transport has increased which enhances Brownian motion, resulting in an increase in thermal conductivity.[28] This Brownian motion caused the particle to collide frequently at a greater rate with the base fluid which increases the heat transfer processes and hence thermal conductivity. Further, this rise in thermal conductivity could also be due to the rise in particle kinetic energy at higher temperatures associated with different interactions like van der Waals and electrostatic forces which had a significant influence on the enhancement of thermal conductivity.[29] It can also be noted, the increase in thermal conductivity of nanofluid with temperature and particle concentration is due to the nature of base fluid.[30] Since in the process of green synthesis water is used as base fluid in most of the work so there is a constant increase in thermal conductivity. This is due to the presence of large number of H-bond in water molecules which can store energy rather transferring it.[31] When the self-stabilized nanoparticles synthesized from any plant extract are added to water it can continuously increase the thermal conductivity depending on the concentration of nanoparticles.[32,33]

The increase in thermal conductivity also depends upon the sonication time of nanofluid. Sonication of nanofluid has been performed for three hours and thermal conductivity was measured at every 30 minutes interval. With increase of sonication time thermal conductivity increased. For increase in sonication time from 30–180 minutes thermal conductivity shows a regular increase in its value from 0.531–0.736 W/mK for the defined volume concentration as shown in Fig. 14(a). The linear regression analysis for accuracy of thermal conductivity of nanofluid with sonication time for different volume concentration is shown in Fig. 14(b). The coefficient of correlation (R^2) value is determined to be 0.8759, 0.9298, 0.9575, 0.908, and 0.9548 for 0.01%, 0.02%, 0.03%, 0.04%, and 0.05% respectively. As the R^2 value is very close to 1, the error fluctuations are very less. The fundamental reason for the enhancement in thermal conductivity by applying the ultrasonication process is that in the event of a sample produced without ultrasonication, particle agglomeration is quite strong, resulting in a bigger

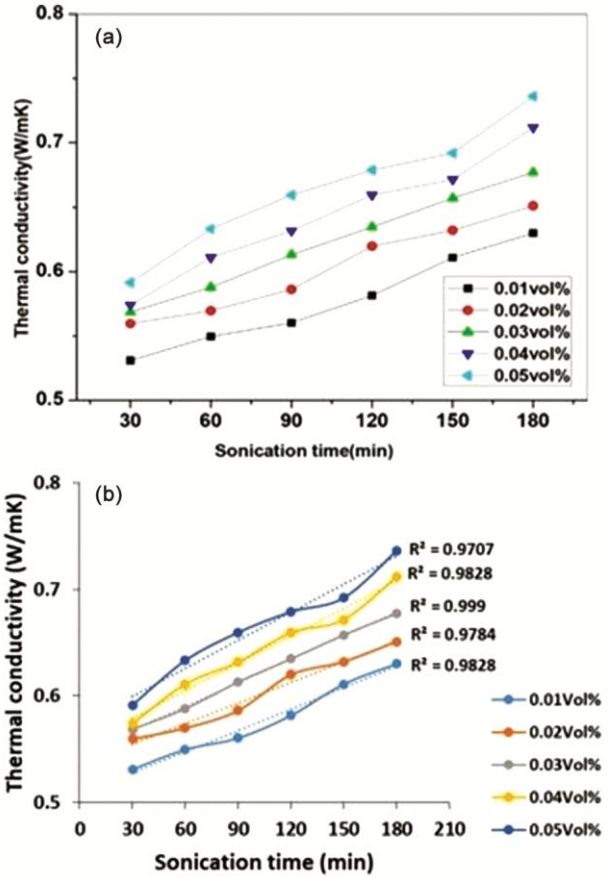

Fig. 14 — Representation of thermal conductivity vs. sonication times; (a) Variation analysis, (b) Regression analysis

cluster and a nanofluid that is not sufficiently homogenized.

Clusters of nanoparticles break down during the ultrasonication process, resulting in uniform dispersion in base fluid which increases the particle mobility and hence increase in thermal conductivity could be observed. This could be due to the homogeneity of nanoparticle dispersion in the base fluid as well as the exceptionally high particle mobility in base fluids. As a result, increasing the sonication period reduced nanoparticle aggregation, resulting in smaller particles and higher thermal conductivity.[34]

Conclusions

Aluminum oxide nanoparticles were successfully synthesized by the green synthesis method using curry leaf extract. Ultrasonic technique was used in the synthesis of both alumina nanoparticles and nanofluid of different volume fractions with less agglomeration, high stability, and dispersion condition. Rhombohedral crystal shape with high crystallinity index confirms the formation of Al_2O_3 nanoparticles of size 38 nm. The morphology analysis at different magnifications confirms the spherical shape of the synthesized Al_2O_3 nanoparticle. The decrease of band gap from 4.8–5.82 eV indicates the reduced shape of the nanoparticles which is confirmed from UV–visible spectra. The spectra of FTIR exhibit the different functional groups with a clear peak for the presence of Al_2O_3 nanoparticles having wave number 604 cm^{-1}. The particle size of 3.12 nm get distributed with maximum probability has been observed from the plots of particle size data. The curve fitting for all the thermophysical properties has been plotted and it was found that in all cases the R^2 value is quite nearer to 1. So it can be said that the experimental results are nearer and well fitted with linear trend line. The rise in thermal conductivity with volume concentration and temperature was confirmed using several nanoparticle characteristic measures. The higher is the sonication time more is the thermal conductivity which is clearly observed from the results of thermal conductivity values. Thus it can be concluded that the current process of nanoparticle synthesis is a green process and has many advantages in the enhancement of thermal conductivity which is quite better than conventional preparation methods.

Nomenclature

Φ	=	Volume fraction
EDS	=	Energy dispersive spectra
FTIR	=	Fourier Transform Infrared Spectroscopy
TEM	=	Transmission Electron microscope
SEM	=	Scanning Electron Microscopy
XRD	=	X-ray Diffraction
	=	Thermal conductivity of nanofluid
	=	Thermal conductivity of base fluid
	=	Enhancement in thermal conductivity
$Al(NO_3)_3$	=	Aluminium nitrate
SiO_2	=	Silicon oxide
N-O	=	Nitrogen –Oxygen bond
Al-O-Al	=	Aluminium–Oxygen bond
	=	Absorption coefficient
	=	Planck's constant (JS)
ν	=	Frequency of ultraviolet light (Hz)
C	=	Energy-independent constant
	=	Optical energy band-gap (eV)
TiO_2	=	Titanium dioxide
Al_2O_3	=	Aluminium oxide

ρ_{nf} Density of nanofluid (Kg/m^3)

ρ_{bf} Density of base fluids (Kg/m^3)

ρ_p Density of nanoparticles (Kg/m^3)

D_{hkl} = Average crystallographic size of reflected phases

k = Scherer's constant

λ = X-ray wavelength (nm),

β_{hkl} = Full width half maximum (FWHM) intensity

θ_{hkl} Bragg's angle (Degree)

Reference

1 Duraisamy P, Green Synthesis of Aluminium Oxide Nanoparticles by using AervaLanta and Terminalia Chebula Extracts, *Int J Res Appl Sci Eng Tech*, **6** (2018) 428–433.

2 Talebi R, Synthesis and characterization of BaWO4 nanoparticles with the aid of different surfactants and their photo catalyst properties, *J Mater Sci*, **28(9) (**2017).

3 Giri R, Ghosh M, Tripathy A & Nath G, Ultrasonic assisted solvent extraction in synthesis of cerianano fluids from rare earth material for heat exchange application, *Adv Nat Sci Nanosci Nanotech*, **12(1)** (2021) 1502.

4 Leena M, Srinivasan S & Prabhaharan M, Evaluation of acoustical parameters and thermal conductivity of TiO_2-ethylene glycol nanofluid using ultrasonic velocity measurements, *Nanotech Review*, **206** (2015) 103–109.

5 Gupta M, Singh V, Kumar R & Said Z, A review on thermophysical properties of nanofluids and heat transfer applications, *Renew Sustain Energy Rev*, **74** (2017) 638–670.

6 Singh K, Sharma S & Gangacharyulu D, Experimental study of thermophysical properties of Al2O3/Water nanofluid, *Int J Res Mech Eng Technol*, **3(2)** (2013) 229–233.

7 Nanda A, Tiadi A, Mallik S K, Giri R & Nath G, Ultrasonic characterization of silver nano fluid, *IOP Conf Ser: Mater Sci Eng*, **360** (2018) 012064.

8 Pastoriza-Gallego M, Lugo L, Legido J & Piñeiro M M, Thermal conductivity and viscosity measurements of ethylene glycol-based AlO nanofluids, *Nanoscale Res Lett*, **(6)** (2011) 221.

9 Sundar L S, Ramana E V, Singh M K & Sousa A C, Thermal conductivity and viscosity of stabilized ethylene glycol and water mixture AlO nanofluids for heat transfer applications: An experimental study, *Int Commun Heat Mass Transf*, **56** (2014) 86–95.

10 Borode A O, Ahmed N A, Olubambi P A, Sharifpur M & Meyer J P, Investigation of the thermal conductivity, viscosity, and thermal performance of graphene nanoplatelet-alumina hybrid nanofluid in a differentially heated cavity, *Front Energy Res*, **9** (2021) 1–15.

11 Said Z & Saidur R, Thermophysical properties of metal oxides nanofluids, nanofluid heat and mass transfer in engineering problems, Mohsen Sheikholeslami Kandelousi, Intech Open, DOI: 10.5772/65610.

12 Elias M M, Mahbubul I M, Saidur R, Sohel M R, Shahrul I M & Khaleduzzaman S S, Experimental investigation on the thermo-physical properties of Al_2O_3 nanoparticles suspended in car radiator coolant, *Int Commun Heat Mass Transf*, **54** (2014) 48–53.

13 Patel H E, Sundararajan T & Das S K, An experimental investigation into the thermal conductivity enhancement in oxide and metallic nanofluids, *J Nanopart Res*, **12** (2009) 1015–1031.

14 Neethumol V, Manjusha H, Benny Cherian A, Sreenivasan P V, Paul J & Asmy Antony K A, PVA-assisted synthesis and characterization of nano α-alumina, *Int J Sci Res*, **4(10)** (2014) 2250–3153.

15 Prashantha P A, Raveendraa R S,Hari Krishna R, Ananda S, Bhagya N P, Nagabhushana B M, Lingaraju K & Raja Naika R, Synthesis, characterizations, antibacterial and photo-luminescence studies of solution combustion-derived α-Al_2O_3 nanoparticles, *J Asian Ceram Soc*, **3** (2015) 345–351.

16 Malviya R K, Verma M & Yadav V, Preparation and characterization of zinc oxide nano fluids in organic components, *Sci Technol Manag J*, **187** (2013) 2738–2740.

17 Hema E, Manikandan A, Karthika P, Antony S A & Venkatraman B R, A novel synthesis of Zn^{2+}-doped $CoFe_2O_4$ spinel nanoparticles: structural, morphological, opto-magnetic and catalytic properties, *J Supercond Nov Magrn*, **28** (2015) 2539–2552.

18 Nagpal S, Nanofluids to be used to make new types of cameras, micro devices, and displays, *Appl Sci*, **11** (2021) 2525.

19 Wilson C A, Experimental Investigation of Nanofluid Oscillating Heat Pipes. *Ph.D. Dissertation, University of Missouri, Columbia, MO, USA*, 2006.

20 Tyagi H, Phelan P & Prasher R, Predicted efficiency of a Low-temperature Nanofluid-based direct absorption solar collector, *J Sol Energy Eng Trans*, **131** (2009) 0410041–0410047.

21 Singh P P & Nath G, Ultrasonic processing and thermo-acoustic analysis of orange peel waste as smart acoustic material: waste and biomass valorization, *Waste Biomass Valor* (2022), https://doi.org/ 10.1007/s12649-022-01699-9.

22 Demetzos C, Application of nanotechnology in imaging & diagnostics, in *Pharmaceutical Nanotechnology: Fundamentals and Practical Applications* (Springer Singapore) 2016, 65–75, ISBN 978-981-10-0791-0.

23 Rodrigues R O, Sousa P, Gaspar J, Bañobre-López M, Lima R & Minas G, Organ-on-a-chip: A preclinical microfluidic platform for the progress of nanomedicine, *Small*, **16(51)** (2020) 2003517.

24 Kung C T, Gao H, Lee C Y, Wang Y N, Dong W, Ko C H, Wang G & Fu L M, Microfluidic synthesis control technology and its application in drug delivery, bioimaging, biosensing, environmental analysis and cell analysis, *Chem Eng J*, **399** (2020) 125748.

25 Esfe, M H, Esfandeh S, Afrand M, Rejvani M & Rostamian S H, Experimental evaluation, new correlation proposing and ANN modeling of thermal properties of EG based hybrid nanofluid containing ZnO-DWCNT nanoparticles for internal combustion engines applications, *Appl Therm Eng*, **133** (2018) 452–463.

26 HemmatEsfe M, Yan W M, Akbari M, Karimipour A & Hassani M, Experimental study on thermal conductivity of DWCNT-ZnO/water-EG nanofluids, *Int Commun Heat Mass Transf*, **68** (2015) 248–251.

27 Malik P, Shankar R & Malik V, Green chemistry based benign routes for nanoparticle synthesis, *J Nanoparticles*, **2014** (2014) 1–14

28 Dwivedi A D & Gopal K, Biosynthesis of silver and gold nanoparticles using Chenopodium album leaf extract, *Colloids Surf A Physicochem Eng Asp*, **369** (2010) 27–33.

29 Kamel M S, Al-Oran O & Lezsovits F, Thermal conductivity of Al_2O_3 and CeO_2 nanoparticles and their

hybrid based water nanofluids: an experimental study, *Periodica Polytechnica Chem Eng*, **65** (2020) 15382–1592.

30 Rostamian S H, Biglari M, Saedodin S & HemmatEsfe M, An inspection of thermal conductivity of CuO-SWCNTs hybrid nanofluid versus temperature and concentration using experimental data, *ANN modeling and new correlation*, *J Mol Liq*, **231** (2017) 364–369.

31 Xuan Y & Li Q, Heat transfer enhancement of nanofluids, *Int J Heat Fluid Flo*, **21** (2000) 58–64.

32 Bidgoli M R, Kolahchi R & Karimi M S, An experimental study and new correlations of viscosity of ethylene glycol-water based nanofluid at various temperatures and different solid concentrations, *Struct Eng Mech*, **58** (2016) 93–102.

33 Gangadevi R & Vinayagam B K, Experimental determination of thermal conductivity and viscosity of different nanofluids and its effect on a hybrid solar collector, *J Therm Anal Calorim*, **136** (2018) 199–209.

34 Chon C H, Kihm K D, Lee S P & Choi S U S, Empirical correlation finding the role of temperature and particle size for nanofluid (AlO) thermal conductivity enhancement, *Appl Phy Lett*, **87** (2005) 153107.